Heliyon 9 (2023) e12885

Contents lists available at ScienceDirect

Heliyon

journal homepage: www.cell.com/heliyon

Research article

The growth and shape of the eyeball and crystalline lens in utero documented by fetal MR imaging

Yingying Hong [a,b,c,1], Li Ning [a,b,c,1], Yang Sun [a,b,c], Huijun Qian [d,**], Yinghong Ji [a,b,c,*]

[a] Eye Institute and Department of Ophthalmology, Eye & ENT Hospital, Fudan University, Shanghai, 200031, China
[b] NHC Key Laboratory of Myopia (Fudan University), Key Laboratory of Myopia, Chinese Academy of Medical Sciences, Shanghai, 200031, China
[c] Shanghai Key Laboratory of Visual Impairment and Restoration, Shanghai, 200031, China
[d] Department of Radiology, Obstetrics and Gynecology Hospital, Fudan University, Shanghai, 200011, China

ARTICLE INFO

Keywords:
Eye biometry
Lens growth
Ocular globe growth
MR imaging
Lens shape
Fetus

ABSTRACT

Purpose: To study the growth model, shape, and developmental relationship of lens and eyeball, we used two-dimensional Magnetic Resonance (MR) imaging to investigate gestationally age-related changes in the selected ocular parameters in vivo.

Materials and methods: We retrospectively reviewed the MR images from 126 fetuses ranging from 21 to 39 weeks' gestation. Ocular parameters on MR imaging of transverse plane were measured including lens diameter (LD), anteroposterior lens diameter (APLD), lens surface area (LS), globe diameter (GD), anteroposterior globe diameter (APGD), globe surface area (GS). The growth model of each biometric against gestational age (GA), aspect ratio of lens and globe (LD/APLD and GD/APGD), and growing relationship between the ratio of lens and globe surface area (LS/GS) were studied by statistical analysis.

Results: The growth model of most biometry for gestational age is logarithmic, except for the diameter of the ocular globe (GD and APGD) showing a quadratic growth pattern. Our study showed that the lens was consistently larger in the transverse than the anteroposterior diameters during 21–39 weeks($P < 0.001$). Besides, the ratio of surface area (LS/GS) was not significantly changing with GA($P = 0.4908$), while the increase of LS was significantly accorded with that of GS($P < 0.001$).

Conclusion: The lens shape throughout fetal life may take part in the process, shape changing from vertical ellipsoid, spherical to transversal ellipsoid, based on the logarithmically increased ratio of lens transverse and anteroposterior diameters. In the meanwhile, the aspect ratio of eyeball in late fetal life may imply a gradually spherical shape during gestation. Nomogram data from this study

Abbreviations: MR, Magnetic Resonance; LD, lens diameter; APLD, anteroposterior lens diameter; LS, lens surface area; GD, globe diameter; APGD, anteroposterior globe diameter; GS, globe surface area; GA, gestational age; US, ultrasound; SNR, signal-to noise ratio; T2W, T2 weighted; CC, correlation coefficient; OLS, ordinary least square; AIC, Akaike Information Criterion; SD, standard deviation; CI, confidence intervals.

* Corresponding author. Eye Institute and Department of Ophthalmology, Eye & ENT Hospital, Fudan University, NHC Key Laboratory of Myopia (Fudan University), Key Laboratory of Myopia, Chinese Academy of Medical Sciences, Shanghai Key Laboratory of Visual Impairment and Restoration, No. 83 Fenyang Road, Shanghai, 200031, China.

** Corresponding author. Department of Radiology, Obstetrics and Gynecology Hospital, Fudan University, No. 419 Fangxie Rd. Shanghai, 200011, China.

E-mail addresses: qianhj79@126.com (H. Qian), jiyh_eent@163.com (Y. Ji).

[1] Co-first authors: Yingying Hong and Li Ning contributed equally to this work.

https://doi.org/10.1016/j.heliyon.2023.e12885
Received 13 October 2022; Received in revised form 6 January 2023; Accepted 6 January 2023
Available online 9 January 2023

may provide appropriate information about morphological changes in the fetal lens and the synchronous relationship between lens and eyeball.

Key summary points

Why carry out this study?

The eyeball and lens growth models in previous researches are varied and lack a uniform standard. Hence, the results of this study used 6 ocular parameters and compared with earlier studies may provide valuable prenatal information about the fetal eyeball and lens.

What was learned from the study?

The lens shape throughout fetal life may take part in the process, shape changing from vertical ellipsoid, spherical to transversal ellipsoid, based on the logarithmically increased ratio of lens transverse and anteroposterior diameters. In the meanwhile, the aspect ratio of eyeball in late fetal life may imply a gradually spherical shape during gestation. Nomogram data from this study may provide appropriate information about morphological changes in the fetal lens and the synchronous relationship between lens and eyeball.

1. Introduction

The lens is a biconvex transparent tissue that is an integral part of the intraocular refractive system, adjusting the size and shape of the lens to focus objects at different distances on the retina [1]. The lens induced from an invagination of surface ectoderm at around 4 weeks gestation can be detected as early as 12–13 weeks of gestation [2,3] when the secondary lens fibers formed after the elongation of epithelial cells near the lens equator [3–6].

Developmental malformation of the lens can lead to congenital cataracts, ectopia lentis, aphakia, and abnormal lens shape or size [7,8]. In addition, because lens development is also affected by adjacent structures [9,10], developmental malformations of the lens are often accompanied by other ocular defects, or as part of a genetic syndrome of multisystem disease [9], [3,5,11]. Fetal ocular biometry is a valuable resource for evaluating fetal growth and detecting congenital abnormalities during pregnancy. Timely and accurate prenatal diagnosis through the abnormality of shape and size of the lens or the eye globe may be an effective way as a warning for potential developmental malformation, especially subtle changes in the brain.

Fetal ultrasound (US) is the first-line modality for detecting and evaluating fetal abnormalities given its wide availability, lack of radiation exposure, and ease of image acquisition. However, US image quality is operator dependent, and affected by fetal position, maternal habits, insufficient amniotic fluid, and/or shadows created by ossified bone. With high-resolution imaging technology development, these limitations can be overcome by using fetal magnetic resonance (MR) imaging. MRI can be a valuable tool to describe normal growth characteristics of the fetal optic system and provided normative data on ocular measurements, as well as detect fetal ocular and lens anomalies such as congenital cataracts, aphakia, hypertelorism, and hypotelorism [12].

Several published MR-based studies of fetal eye measurements employed inconsistent statistical regression models. Harayama et al. [42] described a linear model for fetal eye growth, while Fledelius et al. and his companions [43] proposed an exponential growth model. Still others have discussed secondary growth models of fetal eye growth. More recently, Robinson et al. [2] and Paquette et al. [16] assessed fetal eye growth using MRI in logarithmic and quadratic models, respectively. They propose different standard values for fetal eye measurements. Earlier fetal MR imaging studies, however, lacks the lens measurements and consistent measuring methods, data interpretation, and image acquisition [13–17].

The aim of this study was to determine normal eyeball and lens growth curves in Chinese by in vivo fetal MRI measurements and to compare with the values reported in the literature.

2. Material and methods

2.1. Patients selection

This retrospective study was supervised by both of the ethics committee of the Obstetrics & Gynecology Hospital of Fudan University and the Eye & ENT Hospital of Fudan University. All procedures involving human participants were conducted in full accordance with ethical principles, including the World Medical Association Declaration of Helsinki (version 2002) and the additional requirements of the China. All of the experiments were undertaken with the understanding and written consent of each participants and according to the above-mentioned principles.

From May 2017 to November 2020, the fetal brain MR imaging of fetuses with the gestational age ranging from 21 to 39 weeks were retrospectively collected in Obstetrics & Gynecology Hospital of Fudan University. Pregnancies were dated according to the last menstruation and sonographic data by the obstetricians. The following inclusion criteria were applied to the selection of healthy fetuses used for final analysis: 1) documented two senior radiologists report of an anatomically and developmentally normal fetus, 2) absence of a documented fetal syndromic or chromosomal anomaly, 3) singleton pregnancy, and 4) Chinese parents. Exclusion criteria

were: 1) Any reported congenital abnormality of the fetal brain, face or body, 2) fetuses whose images were assessed visually with poor imaging quality such as severe fetal motion, very low signal-to noise ratio (SNR), image artifacts, or scans with a limited field of view that did not cover the entire fetal head.

The clinical indications for fetal MRI of normal fetuses in this study were based on fetal US findings of suspected brain abnormalities, suspected non-central nervous system abnormalities, suspected small\large head biometry, and suspected fetal growth restriction.

2.2. MR imaging

Fetal MRI was performed on a 1.5 T MR imaging system (Magnetom Avanto, Siemens, Erlangen, Germany) with an 8-channel phased-array body coil. All subjects were scanned in the supine or lateral decubitus position, without sedation. The scanning parameters: half-Fourier-acquisition single-shot turbo spin-echo T2 weighted (T2W) sequences in axial, coronal, and sagittal plane of the fetal brain: TR/TE = 1350/92 ms; section thickness = 4 mm (with 1 mm gap); flip angle = 170°; field of view = 420 × 420 mm^2; matrix size = 320 × 256.

2.3. Measurements

Quantitative measurements were performed on a RadiAnt DICOM Viewer (Medixant company, Poznan, Poland). The transverse plane with the biggest diameter and symmetric morphology of the eyeball was selected to measure ocular parameters. The maximal transverse globe diameter (GD) and lens diameter (LD), anterior–posterior (AP) GD and LD, as well as the area of the cross section of the globe (GS) and lens (LS) were measured for each eye (Fig. 1). The AP was measured between the most anterior point of the cornea

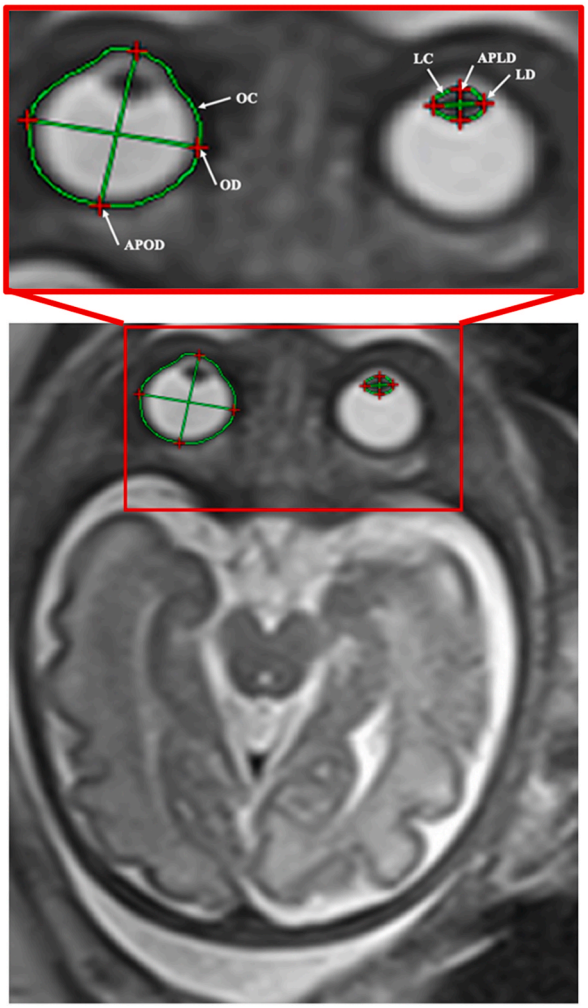

Fig. 1. T2-HASTE MR imaging; Measurement method diagram of globe diameter (GD), anteroposterior (APGD), globe surface area (GS), lens diameters (LD), APLD, and lens surface area (LS) on the transverse MR image with biggest diameter and symmetric morphology of globe.

and the most posterior retinal margins of the eyeballs through the lens center. The GD was measured between the ethmoidal and malar margins of the eyeballs. The GD and AP were always perpendicular in the same subject (Fig. 1). All measurements were performed by a senior professional radiologist who was blinded to gestational age to maintain consistency.

2.4. Statistical analysis

Excel software (Microsoft, WA, USA) was used to store data, and R software version 4.04 (http://www.r-project.org/) was used to perform all statistical analyses. Mean ± Standard Deviation (SD) was used for the statistical description of continuous variables. A Scatter diagram was drawn to determine whether there is a linear relationship, and a two-variable correlation (Pearson's correlation coefficient, CC) combined with a significance test was also performed. The correlation was considered excellent, substantial, moderate, or weak when Pearson's CC values were above 0.75, between 0.75 and 0.60, between 0.60 and 0.40, or less than 0.40, respectively. We performed regression analysis between all the measurements and the GA, including linear, quadratic, and logarithmic statistical evaluation to obtain the "best" fit model when they were compared. The "lm ()" function was used to perform ordinary least square (OLS) regression with the premise of the data with normality, independence, linearity, and homoscedasticity. We used the "bptest ()" function to test whether there is heteroscedasticity and used the Boxcox transition to deal with the heteroscedasticity by determining the lambda (λ) value. Since adding a quadratic term can improve the prediction accuracy of the regression while increasing the formula's complexity, the Akaike Information Criterion (AIC) was used for model comparison, which takes into account the model's statistical fit, and the number of used parameters. A low AIC value indicates that the model has a good fit with fewer parameters. All tests were two-tailed and ***P*** values less than 0.05 were considered to be significant.

Table 1
Nomograms of each measurement for 126 healthy fetuses ranging from 21 to 39 weeks' gestation.

GA	NO.	LD	APLD	LS	GD	APGD	GS
		Mean ± SD (mm)	Mean ± SD (mm)	Mean ± SD (mm)	Mean ± SD (mm)	Mean ± SD (mm)	Mean ± SD (mm)
		95%CI	95%CI	95%CI	95%CI	95%CI	95%CI
21	2	3.35 ± 0.51	2.58 ± 0.46	6.74 ± 1.46	12.05 ± 0.01	10.99 ± 0.48	103.26 ± 4.94
		(-1.23-7.92)	(-1.56–6.71)	(-6.41/19.89)	(12.02–12.08)	(6.67–15.31)	(58.88–147.64)
22	18	3.18 ± 0.24	2.65 ± 0.19	6.48 ± 0.85	12.55 ± 0.69	11.22 ± 0.69	110.72 ± 10.88
		(3.06–3.30)	(2.55–2.74)	(6.05–6.90)	(12.21–12.89)	(10.88–11.57)	(105.31–116.13)
23	15	3.25 ± 0.20	2.64 ± 0.21	6.55 ± 0.81	12.75 ± 0.75	11.36 ± 0.74	113.8 ± 11.67
		(3.14–3.36)	(2.53–2.76)	(6.10–7.00)	(12.34–13.17)	(10.95–11.77)	(107.34–120.26)
24	9	3.43 ± 0.33	2.71 ± 0.26	7.27 ± 1.27	13.41 ± 0.68	12.36 ± 0.81	128.59 ± 13.75
		(3.17–3.68)	(2.52–2.91)	(6.30–8.25)	(12.88–13.94)	(11.74–12.98)	(118.02–139.16)
25	5	3.63 ± 0.31	2.87 ± 0.19	8.28 ± 1.01	14.02 ± 0.86	13.30 ± 1.11	141.94 ± 19.72
		(3.25–4.02)	(2.63–3.11)	(7.02–9.53)	(12.96–15.08)	(11.92–14.68)	(117.4–166.43)
26	9	3.54 ± 0.23	2.74 ± 0.13	7.50 ± 0.76	14.19 ± 0.48	12.96 ± 0.41	137.69 ± 16.14
		(3.37–3.72)	(2.64–2.83)	(6.92–8.09)	(13.82–14.56)	(12.65–13.28)	(125.28–150.10)
27	8	4.04 ± 0.44	2.95 ± 0.31	9.32 ± 1.62	14.64 ± 0.45	13.46 ± 0.55	152.46 ± 10.70
		(3.68–4.41)	(2.69–3.21)	(7.96–10.68)	(14.27–15.01)	(13.00–13.92)	(143.52–161.41)
28	10	4.14 ± 0.49	3.03 ± 0.34	9.92 ± 2.07	15.49 ± 0.85	14.50 ± 0.96	171.71 ± 18.37
		(3.79–4.49)	(2.79–3.28)	(8.43–11.40)	(14.88–16.10)	(13.81–15.18)	(158.57–184.85)
29	7	4.16 ± 0.30	3.11 ± 0.30	9.55 ± 2.87	15.85 ± 0.52	14.74 ± 0.78	176.81 ± 16.90
		(3.89–4.43)	(2.84–3.39)	(6.90–12.21)	(15.36–16.33)	(14.01–15.46)	(161.18–192.44)
30	7	4.49 ± 0.35	3.27 ± 0.31	11.54 ± 1.53	16.14 ± 0.60	15.24 ± 0.58	186.11 ± 10.71
		(4.17–4.82)	(2.99–3.56)	(10.12–12.95)	(15.58–16.70)	(14.70–15.77)	(176.21–196.02)
31	4	4.45 ± 0.32	3.04 ± 0.28	10.70 ± 1.13	16.35 ± 0.54	15.43 ± 0.40	188.64 ± 9.78
		(3.94–4.95)	(2.59–3.49)	(8.90–12.51)	(15.48–17.22)	(14.79–16.07)	(173.08–204.20)
32	8	4.5 ± 0.31	3.23 ± 0.32	11.31 ± 1.64	16.57 ± 0.71	15.77 ± 0.64	197.71 ± 16.36
		(4.24–4.77)	(2.96–3.50)	(9.94–12.68)	(15.97–17.17)	(15.23–16.30)	(184.03–211.39)
33	5	4.88 ± 0.52	3.40 ± 0.31	13.15 ± 2.25	17.10 ± 0.57	16.29 ± 0.63	210.95 ± 12.04
		(4.23–5.52)	(3.02–3.79)	(10.36–15.94)	(16.39–17.81)	(15.50–17.07)	(196.00–225.90)
34	5	5.21 ± 0.22	3.67 ± 0.30	14.82 ± 1.06	17.40 ± 0.44	16.59 ± 0.28	216.85 ± 7.42
		(4.93–5.49)	(3.30–4.04)	(13.50–16.14)	(16.85–17.95)	(16.24–16.94)	(207.64–226.06)
35	4	4.86 ± 0.24	3.12 ± 0.11	11.88 ± 0.40	17.41 ± 0.35	16.47 ± 0.44	218.39 ± 13.07
		(4.49–5.23)	(2.95–3.29)	(11.24–12.51)	(16.85–17.98)	(15.77–17.18)	(197.59–239.19)
36	6	4.93 ± 0.46	3.60 ± 0.47	14.02 ± 2.84	17.58 ± 0.41	16.71 ± 0.32	224.55 ± 6.28
		(4.44–5.42)	(3.11–4.10)	(11.05–17.00)	(17.15–18.00)	(16.37–17.05)	(217.96–231.14)
37	2	5.16 ± 0.28	3.63 ± 0.19	14.74 ± 0.16	18.02 ± 0.74	17.15 ± 0.30	233.65 ± 3.82
		(2.65–7.67)	(1.94–5.31)	(13.31–16.17)	(11.38–24.66)	(12.02–12.08)	(199.33–267.97)
38	1	5.36	3.61	15.72	17.97	17.81	241.10
39	1	4.90	3.30	13.02	18.98	18.68	274.2

Note: No., number, SD, standard deviation; CI, confidence intervals.

3. Results

126 healthy fetuses ranging from 21 to 39 weeks' gestational age met the inclusion criteria (mean 28 ± 5 weeks). Data summary, including mean, standard deviation (SD), and 95% confidence intervals (CI) for GD, APGD, GS, LD, APLD, and LS were displayed in Table 1.

There were no significant differences between left and right eye measurements of the globe ($\boldsymbol{P} > 0.05$) and lens ($\boldsymbol{P} > 0.05$) (paired t-tests). A positive correlation with excellent and substantial Pearson's correlation coefficient between all the variables was observed in Table 2 ($\boldsymbol{P} < 0.001$). A logarithmic growth model was the best fit for most selected parameters (LD, APLD, LS, GD, LD/APLD, and GD/APGD) against GA, while a quadratic growth model appeared to be more fit for the diameter of the eye globe (GD and APGD) (Fig. 2 (a–h)). According to the regression equation, the increases in measurements from 21 to 39 weeks' gestation were approximately 1.8-fold for LD, GD, and APGD, while 1.5-fold for APLD, 2.7-fold for LS, and 2.6-fold for GS. It might be a coincidence that the multiplication of LD (1.8fold) and APLD (1.5fold) happens to be the increment of LS (2.7-fold).

A significant correlation was found between GA and the ratios of the transversal and anteroposterior diameter of lens (LD/APLD) ($R^2 = 0.3790$, $\boldsymbol{P} < 0.001$) and globe (GD/APGD) ($R^2 = 0.3367$, $\boldsymbol{P} < 0.001$) (Fig. 2 (d) and 2(h)). There was no significant correlation between GA and the ratio of lens and globe surface area (LS/GS, $\boldsymbol{P} > 0.4908$), while the surface area of lens was linearly increased with that of the ocular globe ($R^2 = 0.7412$, $P < 0.001$, Fig. 2 (i)). In the terms of lens and eye globe relationship, the growth rate of the former one is less rapid than the latter, as shown in Fig. 2 (j)

The following was found regarding the relationship between LD and APLD: the ratio of the diameter of lens (LD/APLD) was 1.2 at 21week's gestation and 1.5 at 39week′ gestation. The following was found regarding the relationship between GD and APGD: the ratio of the diameter of ocular globe (GD/APGD) was 1.12 at 21weeks′ gestation and 1.03 at 39 weeks' gestation.

The AIC value of each kind of regression model is listed in Supplemental Table 1. The residual standard error, multiple R-squared, adjusted R-squared, F-statistic, P-value, and regression equation of lens and eyeball were summarized in Table 3. The ocular morphology of a normal fetal brain on axial section from this study at 23- and 26-weeks' gestation in two patients showing conical, with angulation of its posterolateral (red arrows) margins (Fig. 3(a) and Fig. 3(b)), respectively. The transversal diameter of lens (LD) measurements from this study were compared and plotted with the data reported in vitro studies (Fig. 4(a)) and in MR imaging, US (Fig. 4(b)). The diameter of ocular globe (GD and APGD) from this study were compared and plotted with the data reported in MR imaging and in vitro studies (Fig. 4(c) and (d), respectively).

4. Discussion

The embryonic development and morphology of lens and eyeball are varied and complicated. The eyeball abnormalities may take alterations forms in size and shape on images, which can be seen as a non-syndrome disease or a part of the multi-systemic disease. The present study supported that MR imaging is an effective way to obtain fetal eye measurement results and establish normatively fetal eye data at 21–39 weeks of gestation to probably guide the clinical evaluation of eye abnormality in utero.

4.1. Comparison with earlier studies

The results of fetal biometry from different studies are varied [13,14,16–26], which may be ascribed to differences in measurement methods, image equipment, and statistical methods. This study supported that the logarithmic growth model was suitable for most ocular parameters against GA, especially the parameters about lens, while the linear globe measurement (GD and APGD) were fitters to a quadratic growth model. Given the discrepancy of embryology and morphology between lens and eye globe, the different growth patterns may be kind reasonable. An MR imaging retrospective study by Li et al. [15] supported the idea that the quadratic growth model was best fit for GD and APGD when three regression models(linear, quadratic, and logarithmic) were considered to curve estimation analyses. Similarly, another study utilizing MRI 3D reconstruction from multiple sets of fast 2D slice acquisitions showed a quadratic model to best fit GD, supporting our results.

However, our results are in contrast to the work by Zhang et al. study [13], where they used 7.0 T postmortem MR imaging, which showed that the globe diameter also logarithmically increases with second trimester. The differences in image technique (including resonance and slice thickness) and the sample gestational age between in vivo and in vitro postmortem MR images may contribute to the inconsistency. In addition, the decreased accuracy of post-mortem MRI for the minor malformation may include anatomical

Table 2
The correlogram between two variables by calculating Pearson's correlation coefficient.

Parameters	GA	GD	APGD	GS	LD	APLD	LS
GA	1.000	0.941	0.941	0.952	0.886	0.745	0.854
GD	0.941	1.000	0.977	0.986	0.886	0.738	0.847
APGD	0.941	0.977	1.000	0.982	0.897	0.754	0.862
GS	0.952	0.986	0.982	1.000	0.891	0.745	0.861
LD	0.886	0.886	0.897	0.891	1.000	0.848	0.962
APLD	0.745	0.738	0.754	0.745	0.847	1.000	0.914
LS	0.854	0.847	0.862	0.861	0.962	0.914	1.000

Note: All $\boldsymbol{P}$ values in the table are less than 0.05.

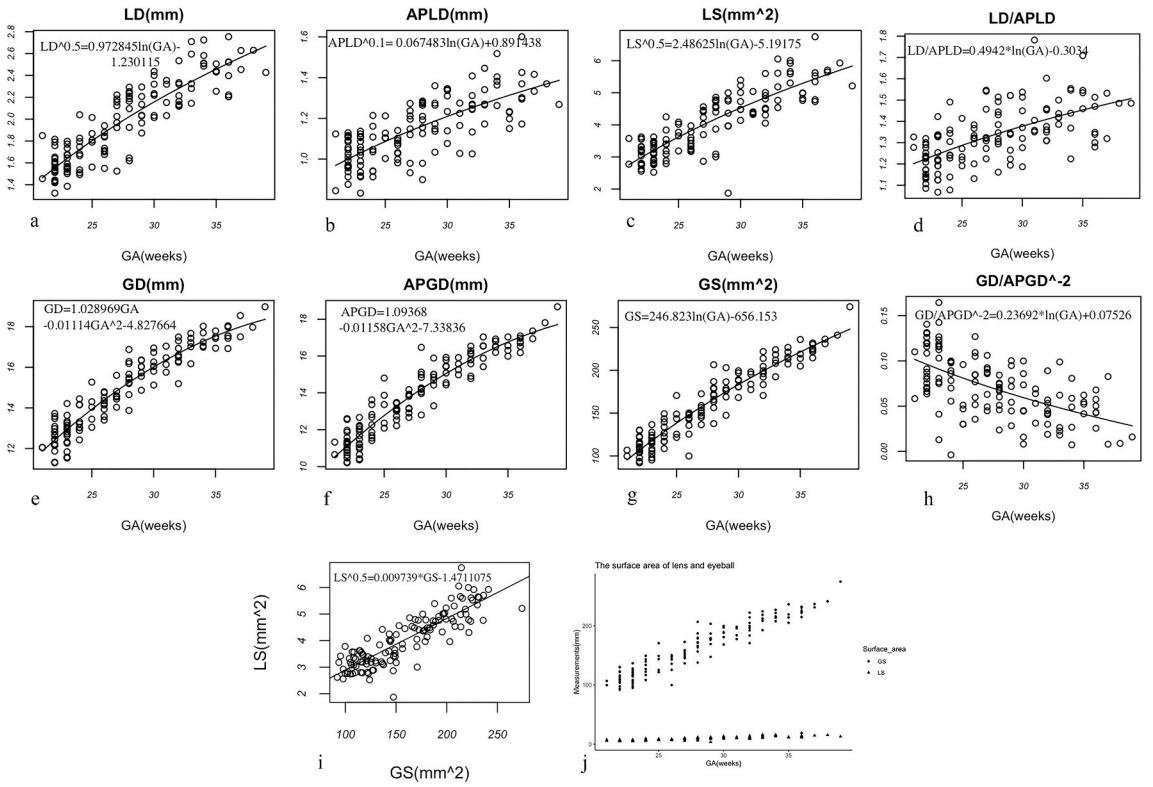

Fig. 2. (a–c) Each lens parameter plotted against their respective growth model [41]. Each ocular globe parameter plotted against their respective growth model. The aspect ratio of (d)lens (LD/APLD) and (h)globe GD/APGD plotted against their respective growth model. **(i)**The relationship between surface area of lens and globe (LS/GS) and (j) the ratio of surface area of lens and globe (LS/GS) plotted against their respective growth model.

Table 3
The summary of regression model between ocular parameters and GA.

Models	Parameters	Residual standard error	Multiple R-squared	Adjusted R-squared	Equation	F-statistic (*P* value)
Logarithmic	$LD^{0.5}$	0.169	0.790	0.789	$LD^{0.5}$ = 0.972845*ln(GA) −1.230115	467.300 (≤0.001)
	$APLD^{0.1}$	0.102	0.555	0.551	$APLD^{0.1}$ = 0.067483 *ln(GA)+0.891438	154.500 (≤0.001)
	$LS^{0.5}$	0.7111	0.7094	1.368	$LS^{0.5}$ = 2.48625* ln(GA)-5.19175	408.7 (≤0.001)
	GD	13.390	0.907	0.906	GS = 246.823 *ln(GA)-656.153	1202.000 (≤0.001)
	LD/APLD	0.1068	0.379	0.374	LD/APLD = 0.4942 *ln(GA)-0.3034	75.680 (≤0.001)
	GD/ $APGD^{-2}$	0.028	0.337	0.331	$GD/APGD^{-2}$ = 0.23692 *ln(GA)+ 0.07526	62.930 (≤0.001)
Quadratic	GD	0.626	0.899	0.898	GD = 1.028969*GA-0.01n114*GA^2-4.827664	549.100 (≤0.001)
	APGD	0 .691	0.899	0.897	APGD = 1.09368–0.01158*GA^2-7.33836	547.000 (≤0.001)

distortion from intrapartum trauma, post-mortem tissue edema, or collapse structures [27], especially when prolonged intra-uterine retention rate and later than 24 h from fetal expulsion [28]. The only other study also including lens diameter in the literature comparable to ours published by Paquette's [16], supporting a similar conclusion(Fig. 4 (b)), however, Zhang et al. [13](in vitro postmortem MRI) and Ehlers et al. [26](in vitro) data was approximately 0.1 cm greater than ours and Paquette's [16] (Fig. 4(a, b)). The possible influential factors have been discussed above.

Fig. 4(b) also compared some earlier US studies in which lens diameters were generally larger than our research partly due to the bony landmarks in US measurements [13]. Fig. 4(c) and (d) have shown a high concordance with earlier MR imaging studies in linear parameters of eye globe (APGD and GD).

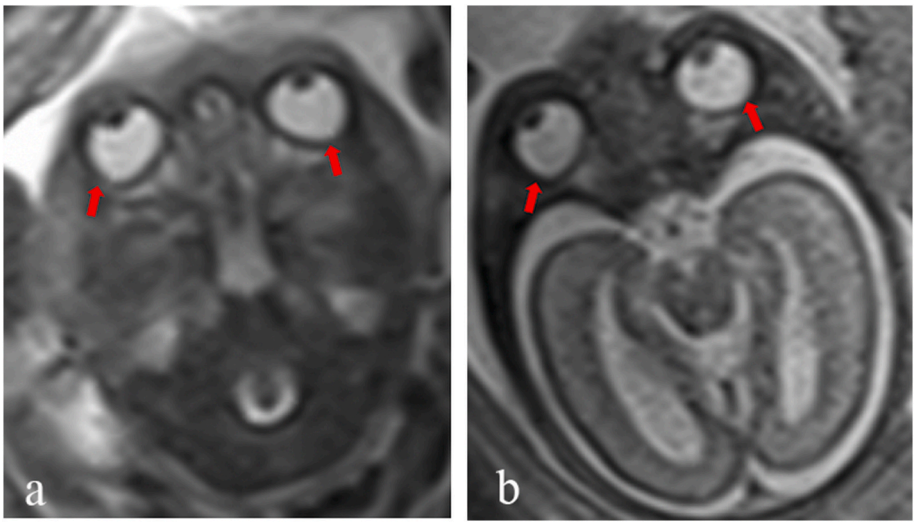

Fig. 3. T2-HASTE MR imaging (TR/TE, 1350 ms/92 ms); the ocular morphology of a normal fetal brain on axial section from this study at (a) 23 and (b) 26 weeks' gestation in two patients, respectively. Note: The globe morphology is conical, with angulation of its posterolateral (red arrows) margins. (For interpretation of the references to colour in this figure legend, the reader is referred to the Web version of this article.)

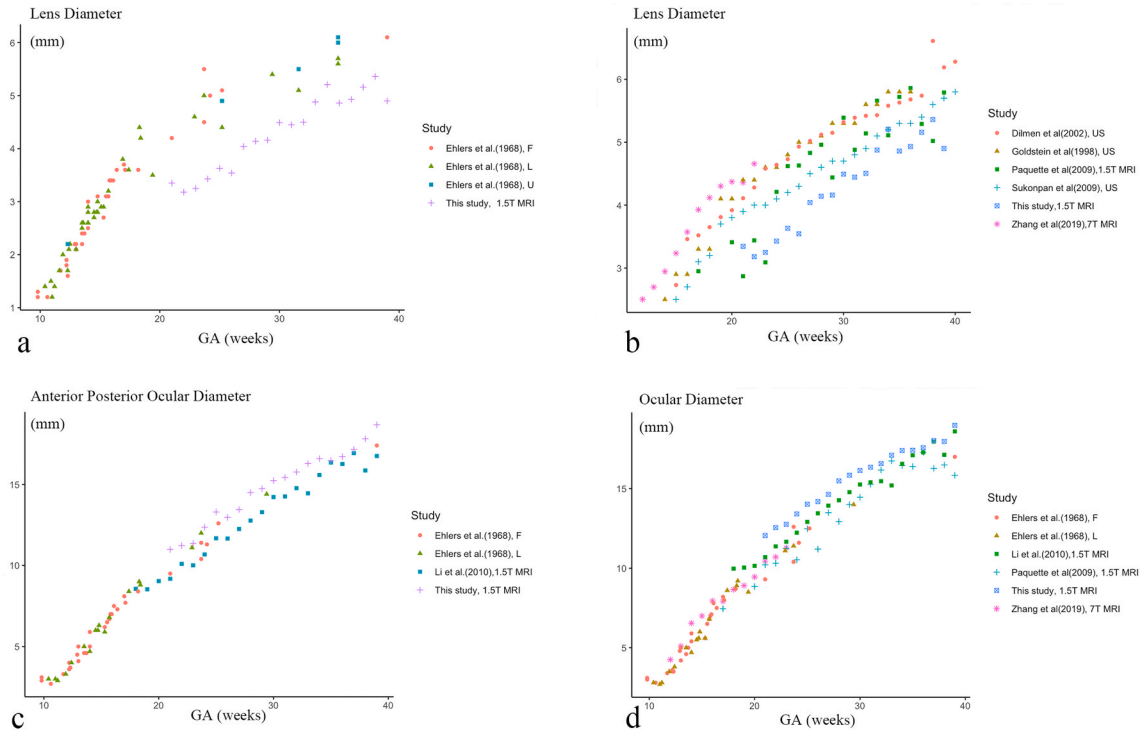

Fig. 4. The diagrams were plotted by comparing with the mean value of ocular parameters in previous studies; the parameters of right eye were chosen only in Ehlers et al. study due to unavailable of the average value; (a) the measurement of LD from this study were compared and plotted with the data from an in vitro study, F(formalin fixed), L(ethanol-formalin-acetic acid fixed, Lillie fixed), U(unfixed); (b) the measurement of lens transversal diameter(LD) from this study were compared and plotted with the data reported in MR imaging and US studies; (c) The measurement of globe anteroposterior diameter(APGD) from this study were compared and plotted with the data reported in MR imaging and in vitro studies; (d) The measurement of globe transversal diameter(GD) from this study were compared and plotted with the data reported in MR imaging and in vitro studies.

4.2. The growth and shape of the eyeball

The early eye morphogenesis may be driven by differential growth, actomyosin contraction, and regional apoptosis, and mediated by physical constraints from adjacent tissue and extracellular matrix [29]. On imaging, the eye globe may take of alteration in size or/and shape if one of the parts is developing irregularly. Therefore, the study may offer a valuable reference tool to help with prenatal diagnosis.

The linear parameter of eye globe (GD and APGD) was quadratically increased with GA, while the surface area of eye globe (GS) was logarithmic, observed in this study. Given our results that the aspect ratio of the globe (GD/APGD) was decreased logarithmically with GA from 1.12 to 1.03 at 21–39 weeks' gestation, we interpret these to mean that the anteroposterior diameter is gradually catching the transversal diameter during pregnancy as time elapsed. Similarly, the in vitro studies [26] had also found that the differences between axial length and diameter of eyeball decreased after about 23rd menstrual week. Herein, we speculated that the eye may begin to be distended in the second trimester by the increased intraocular pressure driven by the growth of eye content. In adults, the axial length is longer than the transversal diameter, indicating the eyeball grows vertically after birth. Owing to the alteration of normal axial length as one of the early signs of eye pathology, including microphthalmia, congenital cataract, and glaucoma [30], importantly, whether the abnormality of the anteroposterior ocular diameter during gestation is associated with the chance of suffering ocular disease after birth need further study.

However, a study investigating the globe morphology on fetal MR imaging showed that it was normal that physical non-spherical globe shape might be conical, with angulation of its posterior and posterolateral margins up to 29 weeks' gestation, and should not be misinterpreted as pathologic [31]. This phenomenon was also found in our MR imaging (Fig. 3). Although we have defined the standard for measuring the diameter (GD and APGD), it was hard to describe the shape of the non-elliptical eyeball in early and mid-pregnancy fetuses by only two diameters.

For example, microphthalmia, which refers to the structurally small eye and may be associated with other ocular disorders, such as anterior and posterior segment disorders, or occurs as a part of syndromes, can be detected during pregnancy by sonographic and MR imaging proved by numerical studies [5,6,8,11,32]. Therefore, the normal eyeball growth can be replenished by these measurement data, but the results in the ratio of GD/APGD may exist misunderstanding in the interpretation of the shape due to the irregularity of globe shape changing during gestation.

4.3. The growth and shape of crystalline lens

As previously described, the human lens is a lifetime growth organ with biphasic pattern to generate two distinct tissue compartments with different properties, including the prenatal formation of nuclear core of fixed dimensions and postnatal ever-expanding cortex [33]. Our result showed that the lens parameters logarithmically increase with GA to further confirm an asymptotic lens growth model in prenatal life.

The aspect ratio (LD/APLD) increased logarithmically with GA from 1.2 to 1.5 during 21–39 weeks' gestation, showing the transversal diameter of lens consistently larger than the anteroposterior diameters.

In addition, based on the formula of the lens aspect ratio, LD/APLD = 0.4942*ln(GA)-0.3034, we found that the anteroposterior diameter of the lens is greater than the transverse before 14 weeks gestation, which was consistent with previous studies in the review literature [34] that showed aspect ratios of lens less than 1.0 between 10 mm and 30 mm stage(about 7–9th weeks) and "almost completely spherical" at 20 mm(about 8th weeks). About the gestation age of 40 weeks, the ratio of LD/APLD (≈1.5) in the present study was similar to the data from a vitro study at birth [33]. These may indicate that the fetal lens might undergo a shape-changing in MR imaging of three stages – vertical ellipsoid (before 13weeks), approximately sphere (14 weeks), and transverse ellipsoid (15 weeks to birth) throughout gestation. However, the result cannot be verified before 21 weeks because the image from early gestational age was lacking in this study due to the restriction of MRI safety.

In the aspect of lens embryology, the onset of secondary fibrogenesis was almost when proliferating cells in monolayer overlying the elongating primary fiber cells [4], at about 7 weeks of gestation [35]. Then, the anterior and posterior lens fibers were elongate more rapidly than the transverse due to the lens polarity at the early stage to generate a vertical lens. As the discrepancy of neo-fiber cell growth rate, the main orientation of lens expansion gradually trans from anterior-posterior to transverse to finally form round ellipsoid. Interestingly, the stage of the approximately spherical lens formation in this study close to the completion of the fetal nucleus (12–14weeks) [35] may indicate some mechanisms that are initiated by the fetal lens accomplished, which probably contribute to the shape-changing. The transverse lens grows mainly because of the continued generation of secondary fibers in late fetal life leading the lens to become increasingly elliptical [36], but the most augmentation was happening in the first two decades after birth [37], especially the first 2–3 years of life with 90% lens equatorial diameter growth [38]. Therefore, it seems rational that the lens shape turns from a round ellipsoid at birth to a flat ellipsoid with aging, which was considered a result of the balance between remodeling and compaction of lens fiber cells during childhood [33,39].

In the terms of lens and eye globe relationship, the growth rate of the former one is less rapid than the latter, as shown in Fig. 2 (j). In addition, the ratio of surface area (LS/GS) in this study was not significantly changing with GA ($\boldsymbol{P} > 0.4908$), while the rising of LS was significantly accorded with that of GS ($LS^{0.5} = 0.009739*GS-1.4711075$, $\boldsymbol{P} < 0.001$, $R^2 = 0.745$), suggesting that there may exist a particular mechanism to maintain the synchronous growth between lens and eyeball, such as equatorial expansion, neural retina, and peripheral mesenchyme [36]. For example, the lens growth slow or defect generally will results in microphthalmia [1], which may contribute to the development of the rest of eye profoundly related to the lens growth process, leading to the decreased volume of ocular globe. Instead, the lens will be mechanically stretched by the equatorial growth to coordinate with the growth of the eyeball to

maintain emmetropia [40].

The crystalline lens, a simple organ but delicate, depends on its correct size and shape, in addition, to fitting properly within the eyeball to perform the optical function to serve as the adjustable focusing element of the eye. Theoretically, congenital lens disease including anomalies and abnormalities of lens size (microphakia and microspherophakia), and shape (lenticonus and spherophakia) can be seen by the imaging technique. Herein, the normal biometry data from this study can potentially assist in disease prenatal diagnosis through forging a meaningful connection between fetal living lens and magnetic resonance imaging.

4.4. Limitations in this study

There are some limitations to our study. Firstly, this is a single-center and retrospective study which is inability to ensure that each fetus has entirely normal ocular globes and the results validated in other healthy and unhealthy fetuses, which requires further longitudinal investigation. The sample is small in the third trimester and lacks first trimester fetuses due to the MR imaging application mainly being a complementary role of US and the strict entry criteria, especially the clear lens images. However, these ocular parameters of our patients were mostly consistent with previous studies. Secondly, motion artifacts and dissolve effects are inevitable, which could cause apparent size and shape alterations. The fact that the section thickness of our image is 4 mm (with 1 mm gap), the chosen plane for the cerebral study does not always correspond to the strict plane of the orbit, and measured by only one radiologist, these may be part of the bias of the study. Some methods to reduce those bias have been taken by the unified measurement standard and the RadiAnt DICOM Viewer software with the tool named “closed polygon” were used, which can deposit nodes around the structure with the advantage of improving the precision by putting the nodes in a more accurate location. In the future, more accurate instruments are needed to further confirm the diagnosis of this part of the potential abnormal-growth children in further researches.

5. Conclusion

In conclusion, the lens shape throughout fetal life may undergo the process, shape changing from vertical ellipsoid, spherical to transversal ellipsoid, based on the logarithmically increased ratio of lens transverse and anteroposterior diameters. In the meanwhile, the aspect ratio of eyeball in late fetal life may imply a gradually spherical shape during gestation. Nomogram data from this study may provide appropriate information about morphological changes in the fetal lens and the synchronous relationship between lens and eyeball.

Author contribution statement

Yingying Hong: Conceived and designed the experiments, Performed the experiments, Analyzed and interpreted the data, Wrote the paper. Li Ning: Performed the experiments, Analyzed and interpreted the data; Wrote the paper. Yang Sun: Analyzed and interpreted the data; Conceived and designed the experiments. Huijun Qian: Conceived and designed the experiments; Performed the experiments; Analyzed and interpreted the data; Contributed reagents, materials, analysis tools or data. Yinghong Ji: Conceived and designed the experiments; Analyzed and interpreted the data; Contributed reagents, materials, analysis tools or data; Wrote the paper.

Funding statement

Dr Yinghong Ji was supported by National Natural Science Foundation of China [81770907, 82070942], Shanghai Talent Development Fund [2018049].

Data availability statement

Data will be made available on request.

Declaration of competing interest

The authors declare that they have no known competing financial interests or personal relationships that could have appeared to influence the work reported in this paper.

Appendix A. Supplementary data

Supplementary data related to this article can be found at https://doi.org/10.1016/j.heliyon.2023.e12885.

References

[1] S. Bassnett, H. Sikic, The lens growth process, Prog. Retin. Eye Res. 60 (2017) 181–200, https://doi.org/10.1016/j.preteyeres.2017.04.001.

[2] A.J. Robinson, S. Blaser, A. Toi, D. Chitayat, S. Pantazi, S. Keating, S. Viero, G. Ryan, MRI of the fetal eyes: morphologic and biometric assessment for abnormal development with ultrasonographic and clinicopathologic correlation, Pediatr. Radiol. 38 (9) (2008) 971–981, https://doi.org/10.1007/s00247-008-0929-3.

[3] C.L. Ondeck, D. Pretorius, J. McCaulley, M. Kinori, T. Maloney, A. Hull, S.L. Robbins, Ultrasonographic prenatal imaging of fetal ocular and orbital abnormalities, Surv. Ophthalmol. 63 (6) (2018) 745–753, https://doi.org/10.1016/j.survophthal.2018.04.006.

[4] J.B. Miesfeld, N.L. Brown, Eye organogenesis: a hierarchical view of ocular development, Curr. Top. Dev. Biol. 132 (2019) 351–393, https://doi.org/10.1016/bs.ctdb.2018.12.008.

[5] A. Searle, P. Shetty, S.J. Melov, T.I. Alahakoon, Prenatal diagnosis and implications of microphthalmia and anophthalmia with a review of current ultrasound guidelines: two case reports, J. Med. Case Rep. 12 (1) (2018) 250, https://doi.org/10.1186/s13256-018-1746-4.

[6] L. Paquette, L. Randolph, M. Incerpi, A. Panigrahy, Fetal microphthalmia diagnosed by magnetic resonance imaging, Fetal Diagn. Ther. 24 (3) (2008) 182–185, https://doi.org/10.1159/000151335.

[7] K.W. Wright, Lens abnormalities, in: K.W. Wright, P.H. Spiegel (Eds.), Pediatric Ophthalmology and Strabismus, Springer New York, New York, NY, 2003, pp. 450–480.

[8] T.Y. Khong, The Special Senses, in: T.Y. Khong, R.D.G. Malcomson (Eds.), Keeling's Fetal and Neonatal Pathology, Springer International Publishing, Cham, 2015, pp. 839–862.

[9] C.J. Thut, R.B. Rountree, M. Hwa, D.M. Kingsley, A large-scale in situ screen provides molecular evidence for the induction of eye anterior segment structures by the developing lens, Dev. Biol. 231 (1) (2001) 63–76, https://doi.org/10.1006/dbio.2000.0140.

[10] H. Sarkar, W. Moore, B.P. Leroy, M. Moosajee, CUGC for congenital primary aphakia, Eur. J. Hum. Genet. 26 (8) (2018) 1234–1237, https://doi.org/10.1038/s41431-018-0171-x.

[11] S. Blazer, E.Z. Zimmer, E. Mezer, M. Bronshtein, Early and late onset fetal microphthalmia, Am. J. Obstet. Gynecol. 194 (5) (2006) 1354–1359, https://doi.org/10.1016/j.ajog.2005.11.010.

[12] D. Bulas, A. Egloff, Benefits and risks of MRI in pregnancy, Semin. Perinatol. 37 (5) (2013) 301–304, https://doi.org/10.1053/j.semperi.2013.06.005.

[13] Z. Zhang, X. Lin, Q. Yu, G. Teng, F. Zang, X. Wang, S. Liu, Z. Hou, Fetal ocular development in the second trimester of pregnancy documented by 7.0 T postmortem Magnetic Resonance Imaging, PLoS One 14 (4) (2019), e0214939, https://doi.org/10.1371/journal.pone.0214939.

[14] C. Velasco-Annis, A. Gholipour, O. Afacan, S.P. Prabhu, J.A. Estroff, S.K. Warfield, Normative biometrics for fetal ocular growth using volumetric MRI reconstruction, Prenat. Diagn. 35 (4) (2015) 400–408, https://doi.org/10.1002/pd.4558.

[15] X.B. Li, G. Kasprian, J.C. Hodge, X.L. Jiang, D. Bettelheim, P.C. Brugger, D. Prayer, Fetal ocular measurements by MRI, Prenat. Diagn. 30 (11) (2010) 1064–1071, https://doi.org/10.1002/pd.2612.

[16] L.B. Paquette, H.A. Jackson, C.J. Tavare, D.A. Miller, A. Panigrahy, Utero eye development documented by fetal MR imaging, AJNR Am J Neuroradiol 30 (9) (2009) 1787–1791, https://doi.org/10.3174/ajnr.A1664.

[17] D.S. Bremond-Gignac, K. Benali, S. Deplus, O. Cussenot, L. Ferkdadji, M. Elmaleh, J.P. Lassau, Utero eyeball development study by magnetic resonance imaging, Surg. Radiol. Anat. 19 (5) (1997) 319–322, https://doi.org/10.1007/BF01637602.

[18] A. Altunkeser, M.K. Korez, Reference ranges for foetal nasal bone length, prenasal thickness, and interocular distance at 18 to 24 weeks' gestation in low-risk pregnancies, BMC Pregnancy Childbirth 17 (1) (2017) 416, https://doi.org/10.1186/s12884-017-1602-3.

[19] K.D. Bojikian, C.R. de Moura, I.M. Tavares, M.T. Leite, A.F. Moron, Fetal ocular measurements by three-dimensional ultrasound, J AAPOS 17 (3) (2013) 276–281, https://doi.org/10.1016/j.jaapos.2013.02.006.

[20] G. Dilmen, A. Köktener, N. Turhan, S. Tez, Growth of the fetal lens and orbit, Int. J. Gynaecol. Obstet. 76 (3) (2002) 267–271, https://doi.org/10.1016/s0020-7292(01)00581-1, the official organ of the International Federation of Gynaecology and Obstetrics.

[21] N. Feldman, Y. Melcer, O. Levinsohn-Tavor, A. Orenstein, R. Svirsky, A. Herman, R. Maymon, Prenatal ultrasound charts of orbital total axial length measurement (TAL): a valuable data for correct fetal eye malformation assessment, Prenat. Diagn. 35 (6) (2015) 558–563, https://doi.org/10.1002/pd.4572.

[22] I. Goldstein, A. Tamir, E.Z. Zimmer, J. Itskovitz-Eldor, Growth of the fetal orbit and lens in normal pregnancies, Ultrasound Obstet. Gynecol. 12 (3) (1998) 175–179, https://doi.org/10.1046/j.1469-0705.1998.12030175.x.

[23] Z. Kivilevitch, L.J. Salomon, B. Benoit, R. Achiron, Fetal interlens distance: normal values during pregnancy, Ultrasound Obstet. Gynecol. 36 (2) (2010) 186–190, https://doi.org/10.1002/uog.7531.

[24] M. Odeh, Y. Feldman, S. Degani, V. Grinin, E. Ophir, J. Bornstein, Fetal eyeball volume: relationship to gestational age and biparietal diameter, Prenat. Diagn. 29 (8) (2009) 749–752, https://doi.org/10.1002/pd.2274.

[25] K. Sukonpan, V. Phupong, A biometric study of the fetal orbit and lens in normal pregnancies, J. Clin. Ultrasound 37 (2) (2009) 69–74, https://doi.org/10.1002/jcu.20537.

[26] N. Ehlers, M.E. Matthiessen, H. Andersen, The prenatal growth of the human eye, Acta Ophthalmol. (Copenh). 46 (3) (1968) 329–349, https://doi.org/10.1111/j.1755-3768.1968.tb02813.x.

[27] S.K. Goergen, E. Alibrahim, N. Govender, A. Stanislavsky, C. Abel, S. Prystupa, J. Collett, S.C. Shelmerdine, O.J. Arthurs, Diagnostic assessment of foetal brain malformations with intra-uterine MRI versus perinatal post-mortem MRI, Neuroradiology 61 (8) (2019) 921–934, https://doi.org/10.1007/s00234-019-02218-9.

[28] G. Izzo, G. Talenti, G. Falanga, M. Moscatelli, G. Conte, E. Scola, C. Doneda, C. Parazzini, M. Rustico, F. Triulzi, A. Righini, Intrauterine fetal MR versus postmortem MR imaging after therapeutic termination of pregnancy: evaluation of the concordance in the detection of brain abnormalities at early gestational stage, Eur. Radiol. 29 (6) (2019) 2740–2750, https://doi.org/10.1007/s00330-018-5878-0.

[29] H.S. Hosseini, L.A. Taber, How mechanical forces shape the developing eye, Prog. Biophys. Mol. Biol. 137 (2018) 25–36, https://doi.org/10.1016/j.pbiomolbio.2018.01.004.

[30] A. Bach, V.M. Villegas, A.S. Gold, W. Shi, T.G. Murray, Axial length development in children, Int. J. Ophthalmol. 12 (5) (2019) 815–819, https://doi.org/10.18240/ijo.2019.05.18.

[31] M.T. Whitehead, G. Vezina, Normal developmental globe morphology on fetal MR imaging, AJNR Am. J. Neuroradiol. 37 (9) (2016) 1733–1737, https://doi.org/10.3174/ajnr.A4785.

[32] D. Song, H. Song, L. Zhou, C. Sun, Q. Wu, D. Li, Prenatal diagnosis of bilateral congenital microphthalmia in two fetuses from the same parents, Indian J. Ophthalmol. 68 (1) (2020) 216–218, https://doi.org/10.4103/ijo.IJO_750_19.

[33] R.C. Augusteyn, On the growth and internal structure of the human lens, Exp. Eye Res. 90 (6) (2010) 643–654, https://doi.org/10.1016/j.exer.2010.01.013.

[34] R. O'Rahilly, The prenatal development of the human eye, Exp. Eye Res. 21 (2) (1975) 93–112, https://doi.org/10.1016/0014-4835(75)90075-5.

[35] Bobrow, Basic and Clinical Science Course (Bcsc) Section 11: Lens and Cataract, 2014, 2014-2015.

[36] V.O.C.S. Cook, F.A. Jakobiec, Duane's Ophthalmology. Vol. Prenatal Development of the Eye and its Adnexa, Lippincott & Williams, 2006. Foundations Volume 1. Ocular Anatomy, Embryology, and Teratology.

[37] E. Martinez-Enriquez, A. de Castro, A. Mohamed, N.G. Sravani, M. Ruggeri, F. Manns, S. Marcos, Age-related changes to the three-dimensional full shape of the Isolated human crystalline lens, Invest. Ophthalmol. Vis. Sci. 61 (4) (2020) 11, https://doi.org/10.1167/iovs.61.4.11.

[38] R. Iribarren, Crystalline lens and refractive development, Prog. Retin. Eye Res. 47 (2015) 86–106, https://doi.org/10.1016/j.preteyeres.2015.02.002.

[39] R.C. Augusteyn, On the contribution of the nucleus and cortex to human lens shape and size, Clin. Exp. Optom. 101 (1) (2018) 64–68, https://doi.org/10.1111/cxo.12539.

[40] D.O. Mutti, K. Zadnik, R.E. Fusaro, N.E. Friedman, R.I. Sholtz, A.J. Adams, Optical and structural development of the crystalline lens in childhood, Invest. Ophthalmol. Vis. Sci. 39 (1) (1998) 120–133.

[41] A. Prince, J. Aguirre-Ghizo, E. Genden, M. Posner, A. Sikora, Head and neck squamous cell carcinoma: new translational therapies, Mt. Sinai J. Med. 77 (6) (2010) 684–699, https://doi.org/10.1002/msj.20216.
[42] K. Harayama, T. Amemiya, H. Nishimura, Development of the cornea during fetal life: comparison of corneal and bulbar diameter, Anat Rec 198 (3) (1980) 531–535, https://doi.org/10.1002/ar.1091980313.
[43] H.C. Fledelius, M. Stubgaard, Changes in eye position during growth and adult life as based on exophthalmometry, interpupillary distance, and orbital distance measurements, Acta Ophthalmol (Copenh) 64 (5) (1986) 481–486, https://doi.org/10.1111/j.1755-3768.1986.tb06958.x.